Available online at www.sciencedirect.com

ScienceDirect

IFAC Papers Online CONFERENCE PAPER ARCHIVE

IFAC PapersOnLine 51-13 (2018) 109–114

On suitable observables for the chaotic Peroxidase-Oxidase autocatalytic reaction

J. M. Méndez-González * **R. Femat** **

* *División de Matemáticas Aplicadas, IPICYT. Camino a la Presa San José 2055, Col. Lomas 4a. sección C.P. 78216. San Luis Potosí, S. L. P., México. (e-mail: jose.mendez@ipicyt.edu.mx).*

** *División de Matemáticas Aplicadas, IPICYT. Camino a la Presa San José 2055, Col. Lomas 4a. sección C.P. 78216. San Luis Potosí, S. L. P., México. (e-mail: rfemat@ipicyt.edu.mx)*

Abstract:
Neurodegenerative diseases such as Alzheimer's and Parkinson present oxidative damage of neurocytes generally caused by reactive oxygen species (ROS). Heme peroxidases consume and produce ROS thus serving as suppresors and promoters of ROS-related pathology. A core reaction network of production and consumption of hydrogen peroxide and superoxide is the Peroxidase-Oxidase (PO). PO reaction was among the first biochemical oscillators to be experimentally and numerically studied, with dynamical scenarios such as multiple steady states, complex oscillations and chaos. In particular, the oxyferrous peroxidase (compound III) and O_2 have been used as observable variables in experiments to record the chaotic dynamics. Moreover, PO reaction has been embedded in nanoparticles in order to serve as a sensor for ROS. In this contribution we quantified, using observability coefficients, which chemical species is more suitable to observe and reconstruct the characteristic complex dynamics of the PO reaction.

Keywords: Chaotic behaviour, Observability indices, Reactive oxygen species, Neurodegenerative diseases, Autocatalysis.

1. INTRODUCTION

Peroxidases are enzymes which catalyze the oxidation of a large class of substrates using H_2O_2. Because peroxidases are able to use O_2 as oxidizing substrate they are also act as oxidases. The catalytic reduction of H_2O_2 to water has an important physiological function because it protects the cell from the toxic oxidative power of H_2O_2, which belongs to the so-called chemically Reactive Oxygen Species (ROS) among others such as superoxide ion radical (O_2^-) and molecular oxygen (O_2). ROS are chemically produced within the cells by means of multiple reaction networks and depending on the cell and tissue types thus playing an important role in cell signaling (Sensse, 2005). The concentration of ROS in an organism may dramatically increase under environmental stress hence damaging cell structures. Neural tissue such as nerve fibrils are susceptible to the increase concentration of ROS that might lead to axonopathy, an early event in different neurodegenerative diseases such as Alzheimer's and Parkinson's (Belenky et al., 2006). Peroxidase-Oxidase (PO) reaction is linked to the appearance of neurodegenerative diseases because of its regulating role as suppressor and promoter of ROS-related pathology (Atamna and Boyle, 2006). This twofold role has been exploited to sensor ROS embedding the PO reaction in nanoparticles (Poulsen et al., 2007).

Since the 70's, PO reaction was among the first biochemical reactions with the capacity to exhibit chaotic oscillations (among other dynamical scenarios) that were experimentally and numerically studied (Aguda and Clarke, 1987; Larter et al., 1987, 1988; Aguda et al., 1989; Steinmetz and Larter, 1991; Bronnikova et al., 1996; Sensse et al., 2006; Olsen, 1983). One of the first proposed reaction network, the so-called BFSO network (Bronnikova et al., 1996) comprised all the dynamical features observed in experiments. Later, Sensse et al. (2006) derived a new reaction network considering six chemical species and thirteen reactions; further reduction lead to a core network of three chemical species: NAD· radical, O_2, and compound III (coIII=Per^{+6}). The addition of a fourth chemical species (O_2^-, Per^{+2} or Per^{+3}) leads to the emergence of Shilnikov chaos provided that these species enter in a supplementary feedback-loop (Sensse and Eiswirth, 2005; Sensse et al., 2006; Sensse, 2005). Thus, we have three subnetworks that share three chemical species and the same route to chaos despite the distinct chemical nature of the fourth chemical species.

Recently, it has been reported that there are kinetic rate constants such that at least one Mass Action Kinetic (MAK) ODE induced by one of the three PO subnetworks can support the same pair of steady states of a second PO subnetwork irrespective of the chemical species being measured (Méndez-González and Femat, 2016). That is, unless we measure the fourth chemical species we cannot distinguish which PO subnetwork is operative or dominant. The biological implications of this redundancy or

10.1016/j.ifacol.2018.07.263

capacity to activate different subnetworks to reach the same steady state values are unknown.

Experimentally, PO chaotic dynamics have been recorded using detectable chemical species such as the oxyferrous peroxidase (coIII=Per^{+6}) and O_2 through their absorbances (Hung and Ross, 1995; Møller et al., 1998). However, it is known that absorbances measurements might hide the contribution of reaction intermediaries to dynamics (Maraun et al., 2004). Furthermore, a frequent scenario in the study of biochemical reaction systems is the presence of fragmentary or unreliable data, thus it is of paramount importance to select properly the chemical species to be measured (*the* observable) to reconstruct the chaotic dynamics of PO subnetworks.

Fortunately, it is assured by Takens' theorem (Takens, 1981) that a single time series contains sufficient information to reconstruct the dynamics of the phase space. A procedure to unfold the dynamic is the proper construction of an equivalent space using the recursive Lie derivatives of an observable variable (*i.e.* a chemical species concentration) (Gilmore and Lefranc, 2002; Letellier et al., 2006). However, this procedure does not guarantee that the chosen observable will be the best among all possible choices: there are better observables than others. The quantification of the degree of observability depending on the variable used can be done it trough the computation of observability coefficients (Letellier et al., 1998; Letellier and Aguirre, 2002; Letellier et al., 2006). These observability coefficients are a local quantity averaged over the (chaotic) attractor, derived from the observability matrix obtained using recursive Lie derivatives of the observable variable as well (Letellier et al., 2006). Comparing the observability coefficients computed for every chemical species it is possible to rank the variables in descending degree of observability (Letellier and Aguirre, 2002; Letellier et al., 2006). In other words, we can quantify which chemical species may influence the quality of a dynamical analysis for the PO reaction under a chaotic regime, for example.

In this contribution we quantified, using observability coefficients, which chemical species is more suitable to observe in order to reconstruct the complex dynamics of the PO reaction. This paper is organised as follows: section 2 presents the MAK ODEs that model all three PO extended reaction networks that exhibit Shilnikov chaos. The construction of the nonlinear observability matrix using Lie derivatives and further derivation of observability coefficients is presented in section 3. Ranking of chemical species depending on their degree of observability is given in section 4. Conclusions are given in section 5.

2. PEROXIDASE-OXIDASE REACTION SUBNETWORKS

According to Sensse et al. (2006), the interplay among the core PO reaction network chemical species, *i.e.*, NAD$\cdot$, O_2 and Per^{+6}, with an additional fourth chemical species, O_2^-, Per^{+2} or Per^{+3}, gives rise to three four dimensional MAK ODEs. We shall denote with capital letter $X_i,\ i = 1\dots4$ the chemical species whereas lower case letters $x_i,\ i = 1\dots4$ stand for chemical species concentrations. Next, we present the associated MAK-ODEs induced by the PO subnetworks and their chaotic behaviour.

2.1 PO subnetwork No. 1

The set of MAK ODEs for the first PO subnetwork as reported by Sensse et al. (2006) is:

$$\begin{aligned}
\dot{x}_1 &= k_1x_1x_3 - k_2x_1x_2 - 2k_3x_1^2 + k_4\\
\dot{x}_2 &= -k_2x_1x_2 - k_5x_2 + k_6 + k_{13}\hat{x}_4^2\\
\dot{x}_3 &= -k_1x_1x_3 - k_7x_3 + k_8\\
\dot{\hat{x}}_4 &= k_2x_1x_2 - 2k_{13}\hat{x}_4^2
\end{aligned} \tag{1}$$

where x_1 =NAD$\cdot$, x_2 =O_2, x_3 =coIII=Per^{+6}, and the fourth species $\hat{x}_4$ =O_2^-. We note, however, that in Sensse et al. (2006) paper the chemical species O_2^- is denoted as x_6. The chaotic attractor obtained from numerical integration of MAK-ODEs (1) is depicted in Fig. 1.

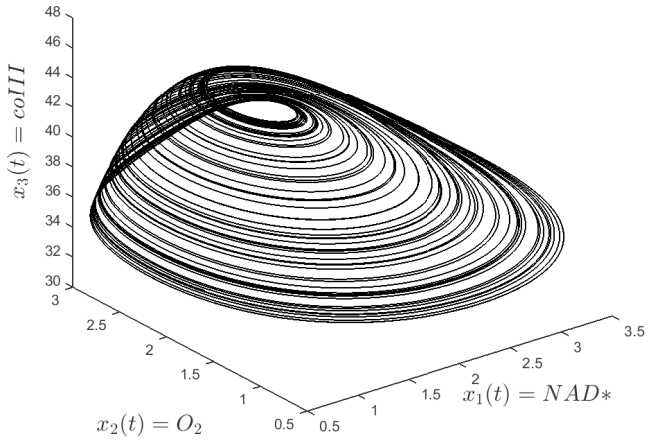

Fig. 1. Chaotic attractor for PO subnetwork No 1. Chemical species: x_1 =NAD$\cdot$, x_2 =O_2, x_3 =coIII=Per^{+6} and $\hat{x}_4$ =O_2^-. Kinetic rate constants for Shilnikov chaos (Sensse et al., 2006): $k_1 = 0.0062, k_2 = 0.415, k_3 = 0.007, k_4 = 0.59, k_5 = 0.14, k_6 = 0.71, k_7 = 0.0001, k_8 = 0.353, k_{13} = 0.0006$.

2.2 PO subnetwork No. 2

The fourth chemical species added to the core PO network is $\tilde{x}_4$ =Per^{+2} (denoted x_5 by Sensse et al. (2006)), which leads to the following MAK ODEs:

$$\begin{aligned}
\dot{x}_1 &= k_1x_1x_3 - k_2x_1x_2 - 2k_3x_1^2 + k_4 - k_{11}x_1\\
\dot{x}_2 &= -k_2x_1x_2 - k_5x_2 + k_6 - k_{12}x_2\tilde{x}_4\\
\dot{x}_3 &= -k_1x_1x_3 - k_7x_3 + k_8 + k_{12}x_2\tilde{x}_4\\
\dot{\tilde{x}}_4 &= k_{11}x_1 - k_{12}x_2\tilde{x}_4
\end{aligned} \tag{2}$$

again with x_1 =NAD$\cdot$, x_2 =O_2, x_3 =coIII=Per^{+6}. Fig. 2 shows the chaotic attractor associated to MAK ODEs (2).

2.3 PO subnetwork No. 3

The addition of x_4 =Per^{+3} to the core PO network gives the following MAK ODEs:

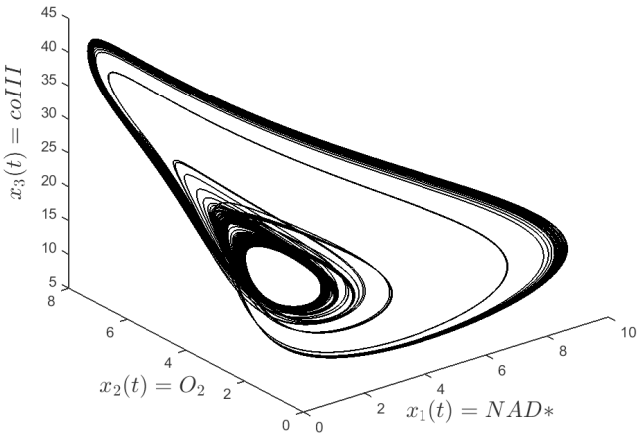

Fig. 2. Chaotic attractor for PO subnetwork No. 2. Chemical species: x_1 =NAD$\cdot$, x_2 =O_2, x_3 =coIII=Per^{+6} and x_4 =Per^{+2}. Kinetic rate constants for Shilnikov chaos (Sensse et al., 2006): $k_1 = 0.032, k_2 = 0.15, k_3 = 0.008, k_4 = 0.0009, k_5 = 0.132, k_6 = 1, k_7 = 0.01, k_8 = 0.59, k_{11} = 0.23, k_{12} = 0.01642$.

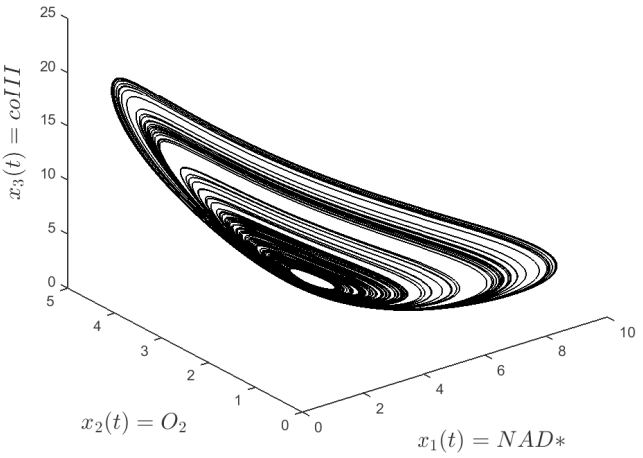

Fig. 3. Chaotic attractor for PO subnetwork No. 3. Chemical species: x_1 =NAD$\cdot$, x_2 =O_2, x_3 =coIII=Per^{+6} and x_4 =Per^{+3}. Kinetic constants for Shilnikov chaos (Sensse et al., 2006): $k_1 = 0.05796, k_2 = 0.3, k_3 = 0.008, k_4 = 0.00525, k_5 = 0.285, k_6 = 1.25, k_7 = 0.001, k_8 = 0.07, k_9 = 0.052, k_{10} = 0.00396$

$$\begin{aligned}
\dot{x}_1 &= k_1 x_1 x_3 - k_2 x_1 x_2 - 2k_3 x_1^2 + k_4 \\
\dot{x}_2 &= -k_2 x_1 x_2 - k_5 x_2 + k_6 \\
\dot{x}_3 &= -k_1 x_1 x_3 - k_7 x_3 + k_8 + k_9 x_4 \\
\dot{x}_4 &= k_1 x_1 x_3 - k_9 x_4 - k_{10} x_4
\end{aligned} \tag{3}$$

Chemical species x_1, x_2 and x_3 are the same as in both previous PO subnetworks. The chaotic attractor for PO subnetwork No. 3 is displayed in Fig. 3.

3. OBSERVABILITY COEFFICIENTS

Let us recall that all three PO subnetworks exhibit chaotic dynamics of Shilnikov type (Sensse, 2005). However, it has been overlooked which chemical species provides a better observability for the dynamics. Thus, it is the purpose of this paper to point out the best observable among the chemical species that conform the chaotic PO subnetworks using the concept of *observability coefficients*.

Briefly, the set of MAK ODEs induced by chemical reaction networks can be written as $\dot{\mathbf{x}} = \mathbf{f}(\mathbf{x}, \mathbf{k})$, where $\mathbf{f}$ is the vector field that maps points from some open set $\mathcal{D} \subset \mathbb{R}^n$ to a tangent space, that is, a space spanned by derivatives. Further, consider the existence of a smooth output function $y = h(\mathbf{x})$, where $h : \mathbb{R}^n \to \mathbb{R}$. In the case of chemical reactions, any measurable chemical species concentration will be valid as an output function. A coordinate transformation (*diffeomorphism*) $\mathbf{z} = \Phi(\mathbf{x})$ around $\mathbf{x}_0$ can be constructed through recursive Lie derivatives as follows (Isidori, 1995; Nijmeijer and van der Schaft, 1995; Slotine and Li, 1991):

$$\mathbf{z} = \Phi(\mathbf{x}) = (h(\mathbf{x}),\ L_f h(\mathbf{x}), \ldots,\ L_f^{s-1} h(\mathbf{x}))^T \tag{4}$$

where s is the dimension of the chemical species concentration vector, $\mathbf{x} = (x_1, \ldots, x_s)$. The Lie derivative of the observable function $y = h(\mathbf{x})$ along the vector field, $\mathbf{f}(\mathbf{x}, \mathbf{k})$, is defined as:

$$L_f h(\mathbf{x}) = \sum_{i=1}^{s} f_i(\mathbf{x}, \mathbf{k}) \frac{\partial h(\mathbf{x})}{\partial \mathbf{x}_i} \tag{5}$$

The jacobian matrix of $\Phi(\mathbf{x})$ defines a more general observability matrix, $\mathbf{J}(\Phi(\mathbf{x})) = \mathcal{Q}(\mathbf{x})$, which becomes the standard observability matrix (Letellier et al., 2006). Considering that $\mathbf{J}(\Phi(\mathbf{x})) = \mathcal{Q}(\mathbf{x})$, Letellier and Aguirre (2002) defined an observability coefficient to quantify a degree of observability as follows:

$$\delta(\mathbf{x}) = \frac{|\lambda_{min}[\mathcal{Q}^T \mathcal{Q}, \mathbf{x}(t)]|}{|\lambda_{max}[\mathcal{Q}^T \mathcal{Q}, \mathbf{x}(t)]|} \tag{6}$$

where the numerator (denominator) of (6) stands for the minimum (maximum) eigenvalue of matrix $\mathcal{Q}^T \mathcal{Q}$ evaluated at point $\mathbf{x}(t)$. As a consequence, the observability coefficient is bounded between $0 \leq \delta(\mathbf{x}) \leq 1$. The lower bound is attained when the system becomes unobservable, that is, when $\mathbf{J}(\Phi(\mathbf{x}))$ is singular because of the local nature of the diffeomorphic map. In other words, as a parameter is varied the dynamical system may gradually become unobservable. Additionally, depending on the singularities of the determinant of the jacobian matrix $\mathbf{J}(\Phi(\mathbf{x}))$ there might be regions in phase space more or less observables than others (Letellier et al., 2006; Letellier and Aguirre, 2010).

Following ideas in (Letellier and Aguirre, 2002) we have the averaged value for $\delta(\mathbf{x})$:

$$\bar{\delta} = \frac{\frac{1}{\tau}\sum_{t=0}^{\tau} \lambda_{min}[\mathcal{Q}^T \mathcal{Q}, \mathbf{x}(t)]}{\frac{1}{\tau}\sum_{t=0}^{\tau} \lambda_{max}[\mathcal{Q}^T \mathcal{Q}, \mathbf{x}(t)]} \tag{7}$$

where τ is the final time considered. Combining the results obtained from Eqs. (6)-(7), the variables used as observables are ranked in descending degree of observability us-

ing the order relation denoted by the symbol "$\triangleright$" (Letellier and Aguirre, 2002). For example, $x_1 \triangleright x_2$ means that x_1 provides a better observability of the underlying dynamics than x_2.

The above computation is implemented in the next section for all chemical species involved in PO subnetworks presented in section 2.

4. RESULTS AND DISCUSSION

For the four dynamical variables of the PO subnetwork No. 1, observability coefficients (and their standard deviation) averaged using Eq. (7) over the chaotic dynamics are:

$$\text{PO subnetwork No. 1} \begin{cases} \bar{\delta}_{x_1} = 3.70 \times 10^{-9} \pm 3.71 \times 10^{-9} \\ \bar{\delta}_{x_2} = 1.09 \times 10^{-9} \pm 1.20 \times 10^{-9} \\ \bar{\delta}_{x_3} = 1.03 \times 10^{-5} \pm 7.47 \times 10^{-6} \\ \bar{\delta}_{x_4} = 3.70 \times 10^{-8} \pm 1.83 \times 10^{-8} \end{cases}$$

From the above coefficient values, we can rank the variables in descending degree of observability according to: $x_3 \triangleright x_4 \triangleright x_1 \triangleright x_2$. The four coefficients have different orders of magnitude which suggest a highly sensitive dependency on the choice of the observable (Letellier and Aguirre, 2002). The chaotic dynamics from PO subnetwork No. 1 is most observable recording the x_3 =coIII=Per^{+6} variable. The worst observable variable corresponds to x_2=O_2, which has been used by Bronnikova et al. (1995) and Møller et al. (1998) to record the chaotic behaviour in experiments; and by Hung and Ross (1995) for deduction and classification of oscillatory mechanisms.

Fig. 4 shows the poorer observability obtained from the differential embedding induced by x_2=O_2: the dynamic is compressed near the domain of $z_2 = \dot{x}_2 = -0.02$, making difficult to distinguish among trajectories. On the contrary, the differential embedding constructed from x_3 =coIII=Per^{+6} leads to a better "unfolding" of the trajectories; regions of compressed dynamics are absent.

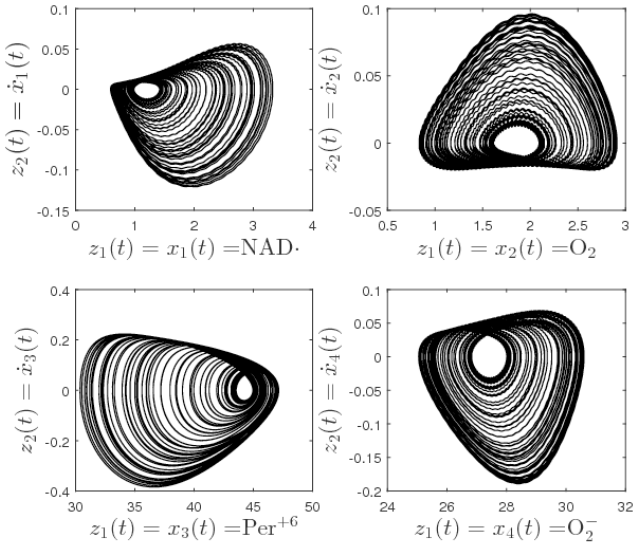

Fig. 4. Differential embeddings produced by the four variables of PO subnetwork No. 1.

With respect to PO subnetwork No. 2 the observable coefficients are:

$$\text{PO network No. 2} \begin{cases} \bar{\delta}_{x_1} = 8.43 \times 10^{-7} \pm 5.88 \times 10^{-6} \\ \bar{\delta}_{x_2} = 1.75 \times 10^{-6} \pm 8.69 \times 10^{-6} \\ \bar{\delta}_{x_3} = 2.94 \times 10^{-5} \pm 7.28 \times 10^{-5} \\ \bar{\delta}_{x_4} = 4.44 \times 10^{-5} \pm 2.01 \times 10^{-4} \end{cases}$$

Thus, the rank of variables is $x_4 \triangleright x_3 \triangleright x_2 \triangleright x_1$. In this case, PO subnetwork No. 2 is more observable from the x_4 =Per^{+2} variable meanwhile x_1 =NAD· will lead to a poor observability of the chaotic regime. The projection of the differential embedding induced by x_1 =NAD· shows a domain around the origin where the dynamics is squeezed, a signature of poor observability (Letellier et al., 2013); see Fig. 5. We point out that the differential embedding produced by x_1 =NAD· is alike (up to a scaling factor) to the differential embedding induced by the variable z in the hyperchaotic Rössler attractor (cf. with Fig. 1 in (Letellier et al., 2005)), suggesting the possibility of a topological equivalence between both dynamical systems.

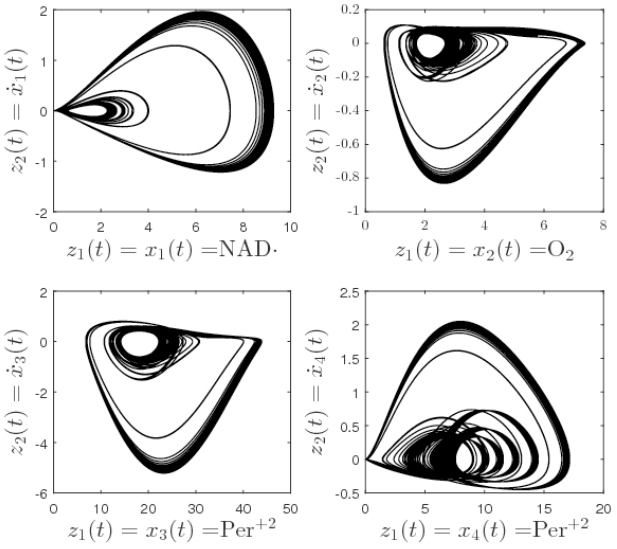

Fig. 5. Differential embeddings produced by the four variables of PO subnetwork No. 2.

Finally, for PO extended network No. 3 the observability coefficients are:

$$\text{PO network No. 3} \begin{cases} \bar{\delta}_{x_1} = 2.15 \times 10^{-6} \pm 4.42 \times 10^{-6} \\ \bar{\delta}_{x_2} = 1.41 \times 10^{-7} \pm 4.29 \times 10^{-7} \\ \bar{\delta}_{x_3} = 4.49 \times 10^{-5} \pm 4.13 \times 10^{-5} \\ \bar{\delta}_{x_4} = 5.09 \times 10^{-4} \pm 8.70 \times 10^{-4} \end{cases}$$

The ranking of variables are: $x_4 \triangleright x_3 \triangleright x_1 \triangleright x_2$. As a consequence of the above averaged values we can conclude that variable x_4 =Per^{+2} provides a better observability of the chaotic dynamics than x_2 =O_2, which remains as the worst observable variable among all three PO extended networks. The differential embeddings are depicted in Fig. 6.

Summing up, we have shown that chemical species x_2 =O_2 is the less appropriate observable to record the chaotic dynamics of the three PO subnetworks. On the contrary, x_4 =Per^{+2} is ranked as the best observable for PO subnetwork No. 2 and 3, whereas x_3 =coIII=Per^{+6} is best for PO

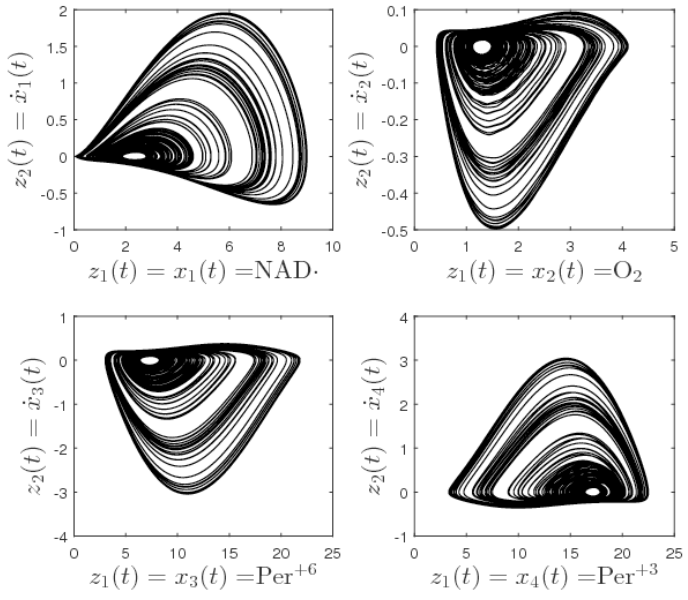

Fig. 6. Differential embeddings produced by the four variables of PO subnetwork No. 3.

subnetwork No. 1. However, let us recall that the fourth chemical species is different in all PO subnetworks. Thus, in order to have a better unfolding of the chaotic dynamics for all three PO subnetworks, the choice of the second best observable chemical species is x_3 =coIII=Per^{+6} which is present in all three PO subnetworks. This decision agrees with the experimental measurements of chaotic dynamics reported by Møller et al. (1998). Furthermore, the aforementioned experiments were performed at 28°C within a pH interval of $5.2 - 6.3$. Hence, the present observability analysis suggest a degree of robustness against pH variations within the chaotic region.

In real biochemical reactions, however, the time evolution of chemical species are always noisy. In theory, the selection of the greater observability coefficients (x_4 =Per^{+2} for PO subnetwork No. 2 and 3; x_3 =coIII=Per^{+6} for PO subnetwork No. 1) provides also a greatness robustness in the presence of noisy data which tends to diminish the degree of observability (Maquet et al., 2004). A further in-depth analysis need to be done for all three PO subnetworks for the ranked observables in order to quantify how the experimental noise affects the chaotic dynamics and its observability.

For example, experimental evidence also suggests that oscillatory dynamics in PO reaction might be a seasonal event (Møller et al., 1998). Nevertheless, the observable chemical species used to argue seasonal oscillations was x_2 =O_2 (Møller et al., 1998), which the present observability analysis ranked it as the worst to analyse PO reaction dynamics. Further studies are required to determine if such seasonal event is the product of the interaction between experimental noise and the intrinsic oscillatory dynamics, or the selection of x_2 =O_2 as the observable to unfold the chaotic dynamics.

5. CONCLUSIONS

Using the concept of observability coefficients, we have shown that, in the presence of noise-free data, chemical species x_2 =O_2 is the less appropriate observable to record the chaotic dynamics of the three chaotic PO subnetworks. Chemical species x_4 =Per^{+2} was ranked as the more convenient observable for PO subnetwork No. 2 and 3, whereas chemical species x_3 =coIII=Per^{+6} is best for PO subnetwork No. 1.

REFERENCES

Aguda, B.D. and Clarke, B.L. (1987). Bistability in chemical reaction networks: Theory and application to the peroxidase-oxidase reaction. *J. Chem. Phys.*, 87, 3461. doi:http://dx.doi.org/10.1063/1.452991.

Aguda, B.D., Larter, R., and Clarke, B.L. (1989). Dynamic elements of mixed mode-oscillations and chaos in a peroxidase-oxidase model network. *J. Chem. Phys.*, 90, 4168. doi:http://dx.doi.org/10.1063/1.455774.

Atamna, H. and Boyle, K. (2006). Amyloid-β peptide binds with heme to form a peroxidase: Relationship to the cytopathologies of alzheimers disease. *Proc. Natl. Acad. Sci. USA*, 103(9), 3381–3386. Doi:10.1073/pnas.0600134103.

Belenky, P., Bogan, K.L., and Brenner, C. (2006). NAD* metabolism in health and disease. *Trends in biochemical sciences*, 32(1), 12–19. doi:10.1016/j.tibs.2006.11.006.

Bronnikova, T.V., Fed'kina, V.R., Schaffer, W.M., and Olsen, L.F. (1995). Period-doubling bifurcations and chaos in a detailed model of the peroxidase-oxidase reaction. *J. Phys. Chem.*, 99(23), 9309–9312. doi: 10.1021/j100023a001.

Bronnikova, T.V., Schaffer, W.M., and Olsen, L.F. (1996). Quasiperiodicity in a detailed model of the peroxidase-oxidase reaction. *J. Chem. Phys.*, 105, 10849. doi: http://dx.doi.org/10.1063/1.472927.

Gilmore, R. and Lefranc, M. (2002). *The topology of chaos. Alice in stretch and squeezeland.* John Wiley and Sons, Inc., 1st edition.

Hung, Y.F. and Ross, J. (1995). New experimental methods toward the deduction of the mechanism of the oscillatory peroxidase-oxidase reaction. *J. Phys. Chem.*, 99(7), 1974–1979. doi:10.1021/j100007a030.

Isidori, A. (1995). *Nonlinear control systems.* Springer–Verlag, 3rd. edition.

Larter, R., Bush, C.L., Lonis, T.R., and Aguda, B.D. (1987). Multiple steady states, complex oscillations, and the devil's staircase in the peroxidase-oxidase reaction. *J. Chem. Phys.*, 87, 5765. doi: http://dx.doi.org/10.1063/1.453550.

Larter, R., Steinmetz, C.G., and Aguda, B.D. (1988). Fast-slow variable analysis of the transition to mixed-mode oscillations and chaos in theperoxidase reaction. *J. Chem. Phys.*, 89, 6506. doi: http://dx.doi.org/10.1063/1.455370.

Letellier, C., Denis, F., and Aguirre, L. (2013). What can be learned from a chaotic cancer model? *J. Theor. Biol.*, 322, 7–16. doi: http://dx.doi.org/10.1016/j.jtbi.2013.01.003.

Letellier, C., Maquet, J., Sceller, L.L., Gouesbet, G., and Aguirre, L.A. (1998). On the non-equivalence of observables in phase-space reconstructions from recorded

time series. *J. Phys. A: Math. Gen.*, 31(39), 7913. doi: http://dx.doi.org/10.1088/0305-4470/31/39/008.

Letellier, C., Aguirre, L., and Maquet, J. (2006). How the choice of the observable may influence the analysis of nonlinear dynamical systems. *Commun. Nonlinear Sci. Numer. Simul.*, 11(5), 555–576. doi: http://dx.doi.org/10.1016/j.cnsns.2005.01.003.

Letellier, C. and Aguirre, L.A. (2002). Investigating nonlinear dynamics from time series: The influence of symmetries and the choice of observables. *Chaos*, 12(3), 549–558. doi:http://dx.doi.org/10.1063/1.1487570.

Letellier, C. and Aguirre, L.A. (2010). Interplay between synchronization, observability, and dynamics. *Phys. Rev. E*, 82, 016204. doi:10.1103/PhysRevE.82.016204.

Letellier, C., Aguirre, L.A., and Maquet, J. (2005). Relation between observability and differential embeddings for nonlinear dynamics. *Phys. Rev. E*, 71, 066213. doi: 10.1103/PhysRevE.71.066213.

Maquet, J., Letellier, C., and Aguirre, L.A. (2004). Scalar modeling and analysis of a 3d biochemical reaction model. *J. Theor. Biol.*, 228(3), 421 – 430. doi: http://dx.doi.org/10.1016/j.jtbi.2004.02.004.

Maraun, D., Horbelt, W., Rust, H., Timmer, J., Happersberger, H.P., and Drepper, F. (2004). Identification of rate constants and nonobservable absorption spectra in nonlinear biochemical reaction dynamics. *Int. J. Bifurcation Chaos*, 14(06), 2081–2092. doi: 10.1142/S0218127404010473.

Méndez-González, J. and Femat, R. (2016). Steady state equivalence among autocatalytic peroxidase-oxidase reactions. *J. Chem. Phys.*, 145, 225101. doi: 10.1063/1.4968554.

Møller, A.C., Hauser, M.J., and Olsen, L.F. (1998). Oscillations in peroxidase-catalyzed reactions and their potential function in vivo. *Biophys. Chem.*, 72(1-2), 63 – 72. doi:http://dx.doi.org/10.1016/S0301-4622(98)00123-9.

Nijmeijer, H. and van der Schaft, A.J. (1995). *Nonlinear dynamical control systems*. Springer–Verlag, 3rd edition.

Olsen, L.F. (1983). An enzyme reaction with a strange attractor. *Phys. Lett. A*, 94(9), 454–547. doi: 10.1016/0375-9601(83)90853-8.

Poulsen, A.K., Scharff-Poulsen, A.M., and Olsen, L.F. (2007). Horseradish peroxidase embedded in polyacrylamide nanoparticles enables optical detection of reactive oxygen species. *Analytical Biochemistry*, 366, 29–36. doi:10.1016/j.ab.2007.04.004.

Sensse, A. (2005). *Convex and toric geometry to analyze complex dynamics in chemical reaction systems*. Ph.D. thesis, Otto-von-Guericke-Universitat, Magdeburg.

Sensse, A. and Eiswirth, M. (2005). Feedback-loops for chaos in activator-inhibitor systems. *J. Chem. Phys.*, 122, 44516. doi:doi:10.1063/1.1840511.

Sensse, A., Hauser, M.J.B., and Eiswirth, M. (2006). Feedback loops for shil'nikov chaos: The peroxidase-oxidase reaction. *J. Chem. Phys.*, 125, 014901. doi: http://dx.doi.org/10.1063/1.2207140.

Slotine, J.J.E. and Li, W. (1991). *Applied nonlinear control*. Prentice-Hall.

Steinmetz, C.G. and Larter, R. (1991). The quasiperiodic route to chaos in a model of the peroxidase-oxidase reaction. *J. Chem. Phys.*, 94, 1388. doi: http://dx.doi.org/10.1063/1.459996.

Takens, F. (1981). Detecting strange attractors in turbulence. In D. Rand and L.S. Young (eds.), *Dynamical Systems and Turbulence, Warwick 1980*, volume 898 of *Lecture Notes in Mathematics*, 366–381. Springer Berlin Heidelberg. doi:10.1007/BFb0091924.